



CaAlSiN₃:Eu/glass composite film in reflective configuration

A thermally robust and efficient red-emitting color converter with high saturation threshold for high-power high color rendering laser lighting

Xu, Jian; Yang, Yang; Jiang, Zhi; Hu, Baofu; Wang, Xinliang; Ji, Haipeng; Wang, Jian; Guo, Ziquan; Du, Baoli; Dam-Hansen, Carsten

Total number of authors:

11

Published in:

Ceramics International

Link to article, DOI:

[10.1016/j.ceramint.2021.02.094](https://doi.org/10.1016/j.ceramint.2021.02.094)

Publication date:

2021

Document Version

Peer reviewed version

[Link back to DTU Orbit](#)

Citation (APA):

Xu, J., Yang, Y., Jiang, Z., Hu, B., Wang, X., Ji, H., Wang, J., Guo, Z., Du, B., Dam-Hansen, C., & Jensen, O. B. (2021). CaAlSiN₃:Eu/glass composite film in reflective configuration: A thermally robust and efficient red-emitting color converter with high saturation threshold for high-power high color rendering laser lighting. *Ceramics International*, 47(11), 15307-15312. <https://doi.org/10.1016/j.ceramint.2021.02.094>

General rights

Copyright and moral rights for the publications made accessible in the public portal are retained by the authors and/or other copyright owners and it is a condition of accessing publications that users recognise and abide by the legal requirements associated with these rights.

- Users may download and print one copy of any publication from the public portal for the purpose of private study or research.
- You may not further distribute the material or use it for any profit-making activity or commercial gain
- You may freely distribute the URL identifying the publication in the public portal

If you believe that this document breaches copyright please contact us providing details, and we will remove access to the work immediately and investigate your claim.

1 **CaAlSiN₃:Eu/glass composite film in reflective configuration: a**
2
3 **thermally robust and efficient red-emitting color converter with high**
4
5 **saturation threshold for high-power high color rendering laser lighting**
6
7

8 Jian Xu^a, Yang Yang^a, Zhi Jiang^a, Baofu Hu^a, Xinliang Wang^{a,*}, Haipeng Ji^b, Jian
9
10 Wang^a, Ziquan Guo^{c,*}, Baoli Du^a, Carsten Dam-Hansen^d, Ole B. Jensen^d
11
12

13
14 ^a*Lab of New Energy Materials and Devices, School of Physics and Electronic Information, Henan*
15
16 *Polytechnic University, Jiaozuo 454000, China*
17

18
19
20 ^b*School of Materials Science and Engineering, Zhengzhou University, Zhengzhou 450001, China*
21

22
23 ^c*Fujian Engineering Research Center for Solid-State Lighting, Department of Electronic Science,*
24
25 *Xiamen University, Xiamen 361005, China*
26

27
28 ^d*Diode Lasers and LED Systems Group, Department of Photonics Engineering, Technical University*
29
30 *of Denmark, Roskilde 4000, Denmark*
31
32

33
34
35
36 **ABSTRACT**
37

38
39 To achieve high color rendering and proper color temperature, a red color converter is
40
41 essential for phosphor-converted white lighting devices. CaAlSiN₃:Eu²⁺ (CASN) is a
42
43 highly suitable red phosphor for white light-emitting diodes. However, it can be hardly
44
45 used in high-power laser lighting due to poor thermal/chemical performance of the
46
47 phosphor/silicone resin mixture. A series of all-inorganic CASN-based phosphors (e.g.,
48
49 composite ceramic and phosphor-in-glass) were developed to avoid the use of resin.
50
51 However, new challenges emerged: none of them showed sufficient luminous efficacy
52
53 (i.e., >50 lm/W) and adequate saturation-threshold (i.e., >30 W or 10 W/mm²). Here,
54
55
56
57
58
59
60

1 we report a facile fabrication of CASN/glass composite films using a simple and
2
3 efficient blade-coating method. Upon 450 nm excitation, the resultant composite film
4
5 presents a high internal quantum efficiency of ~83%, comparable to that of pristine
6
7 CASN powder (~90%). When irradiated with a blue laser, the composite film shows a
8
9 record high luminous efficacy of 82 lm/W. Furthermore, its saturation threshold was
10
11 investigated in high power and high power density mode, respectively. When measured
12
13 in high power mode, it shows a high saturation threshold over 29.7 W (1.75 W/mm²),
14
15 thus achieving a high luminous flux of 1576 lm; when measured in high power density
16
17 mode, it shows a saturation threshold of ~10.2 W/mm² (1.13 W). With abovementioned
18
19 excellent properties, the CASN/glass composite film has great potential for use in high-
20
21 power and high color rendering laser lighting.
22
23
24
25
26
27
28
29
30

31 **Keywords:** Laser lighting; CaAlSiN₃:Eu; Reflective configuration; Saturation threshold;
32
33 Composite film
34
35
36
37
38

39 1. Introduction

40
41
42 Compared with light-emitting diodes (LEDs), laser diodes (LDs) can maintain
43
44 higher wall-plug efficiency at a high current density (i.e., 30 kA/cm²) and have a much
45
46 smaller emitting area [1-4]. These favorable properties enable LD-based white-light
47
48 sources to achieve very high luminance and illuminance; therefore, they have a
49
50 promising future in applications like searchlights, auto headlamps, projectors, and street
51
52 lamps. Similar to white LEDs, commercial white LDs are usually made from a blue LD
53
54 chip and phosphor(s) [4-8]. Thus, phosphors are one of the key components and
55
56
57
58
59
60
61
62
63
64
65

1 significantly affect the colorimetric and photometric properties of white LEDs.
2

3 Conventional white LED encapsulation scheme involves the use of organic
4 bonding materials (e.g., epoxy resin and silicone); they are mixed with phosphor
5 powder and coated on the LED wafer. This scheme is, however, not applicable in laser
6 lighting because organic packaging materials cannot withstand laser irradiation [6, 7,
7 9-11]. To accommodate the distinguishing features of LEDs, a series of all-inorganic
8 encapsulation schemes were explored, including phosphor-in-glass (PiG), phosphor
9 ceramic, single crystal, and phosphor film [9, 12-23]. Many of these phosphors are
10 capable of withstanding high power laser irradiation. So far, most of these all-inorganic
11 phosphors are based on Ce^{3+} -doped $\text{Y}_3\text{Al}_5\text{O}_{12}$ (YAG:Ce). As a canonical yellow-
12 emitting phosphor, YAG:Ce has many favorable properties such as fast luminescence
13 decay time (~70 ns), efficient absorption of blue light (~455 nm), high external quantum
14 efficiency (EQE >70%), and a broad emission band in the visible region [19, 24-27].
15 However, it is very difficult to achieve adequate color rendering index (CRI) and proper
16 correlated color temperature (CCT) for lighting devices based on only YAG:Ce
17 phosphor due to the deficiency of red emission component.
18
19

20 $\text{CaAlSiN}_3:\text{Eu}^{2+}$ (CASN) is a highly suitable red-emitting phosphor that can
21 effectively compensate the deficiency of red light of YAG:Ce [11, 12, 28-33]. Several
22 types of all-inorganic CASN-based phosphors have been developed to improve the
23 colorimetric properties of white LEDs. Zhu et al. developed a CASN-based PiG; however,
24 it got saturated at only 0.5 W/mm^2 [29]. Zhang et al. recently reported a CASN-based
25 PiG where the saturation threshold reached 1.90 W/mm^2 . However, the maximum
26
27
28
29
30
31
32
33
34
35
36
37
38
39
40
41
42
43
44
45
46
47
48
49
50
51
52
53
54
55
56
57
58
59
60
61
62
63
64
65

1 luminous flux was only 49 lm [12]. Remarkable progress was made by Li et al.; they
2
3 fabricated a CASN-based phosphor ceramic with a high luminous efficacy of 42 lm/W.
4
5 Furthermore, a saturation threshold of 2 W/mm² and a maximum luminous flux of ~205
6
7 lm were achieved [30, 33]. Further progress was made by Xu et al. who recently
8
9 reported a CASN/glass composite film operating in transmission configuration. The
10
11 composite film achieved an improved saturation threshold of 3.2 W/ mm² (12.7 W),
12
13 and the maximum luminous flux reached 189 lm [28]. Considering that the saturation
14
15 threshold of YAG:Ce-based phosphors could be increased to higher than 10 W/mm² (or
16
17 30 W) [8, 11, 13, 15, 19, 24, 25], the saturation threshold of CASN-based phosphor is
18
19 expected to match with that of YAG:Ce. Unfortunately, despite the continuous progress
20
21 made in this field, current CASN-based phosphors still did not achieve the desired
22
23 saturation threshold.
24
25
26
27
28
29
30
31

32
33
34 Several reasons can be attributed to the insufficient saturation threshold of CASN-
35
36 based phosphors. First, the luminescence decay of Eu²⁺ is relatively slow (~1 μs) [4, 6,
37
38 32]. Second, the Stokes loss is relatively large when converting blue light to red. Third,
39
40 the co-firing process frequently involves the use of glass, corroding the CASN and
41
42 introducing a luminescence quencher (i.e., Eu³⁺) [4, 6, 7, 34]. Lastly, thick samples
43
44 usually suffer from poor thermal conduction; it is very difficult to machine bulk PiG
45
46 and ceramic to thinner than 150 μm (due to the brittleness). Considering that the Stokes
47
48 loss and luminescence decay for a certain phosphor are intrinsic, the improvement
49
50 measures should focus on the annealing strategy and thermal conduction management.
51
52
53
54
55
56
57

58
59 A survey of CASN-based phosphors conducted with these features in mind led us
60
61
62
63
64
65

1 to focus on the CASN/glass composite film in reflective configuration. Compared to
2
3 CASN-based ceramic and PiG, a composite film can be much thinner ($<50\ \mu\text{m}$) and
4
5 therefore effectively facilitate heat dissipation. Compared to a composite film in
6
7 transmission configuration, the distance from the laser irradiation spot to heat sink for
8
9 the reflective configuration is obviously shorter, which can also benefit for dissipating
10
11 heat. Furthermore, using a SnO-P₂O₅-ZnO glass, the annealing temperature can be
12
13 reduced to 470 °C; thus, a CASN/glass composite film can maintain a high internal
14
15 quantum efficiency (IQE) of ~83% (92% of that of pristine powder). With above
16
17 favorable features, the resulting composite film shows a record high luminous efficacy
18
19 of 82 lm/W. The laser-driven colorimetric and photometric properties were investigated
20
21 in high power mode and high power density mode, respectively. A typical sample shows
22
23 a saturation threshold of more than 29.7 W (1.75 W/mm²) for high power mode and
24
25 10.2 W/mm² (1.13 W) for high power density mode. These findings give us reasons to
26
27 believe that this study will not only provide a robust and efficient CASN-based red
28
29 phosphor for high-power laser lighting, but also provide valuable guidelines for
30
31 improving the luminous efficacy and saturation threshold of other nitride phosphors.
32
33
34
35
36
37
38
39
40
41
42
43
44
45
46

47 **2. Experimental**

48 **2.1 Fabrication of CASN/glass composite film**

49
50 A viscous ink was made by mixing a glass powder (SnO-P₂O₅-ZnO, $T_g \approx 390\ \text{°C}$),
51
52 CASN powder (Yantai Shield, SDR-630), and organic vehicle. The weight of CASN
53
54 phosphor was fixed at 1 g. The “glass to phosphor” (hereafter denoted as “GtP”) weight
55
56
57
58
59
60
61
62
63
64
65

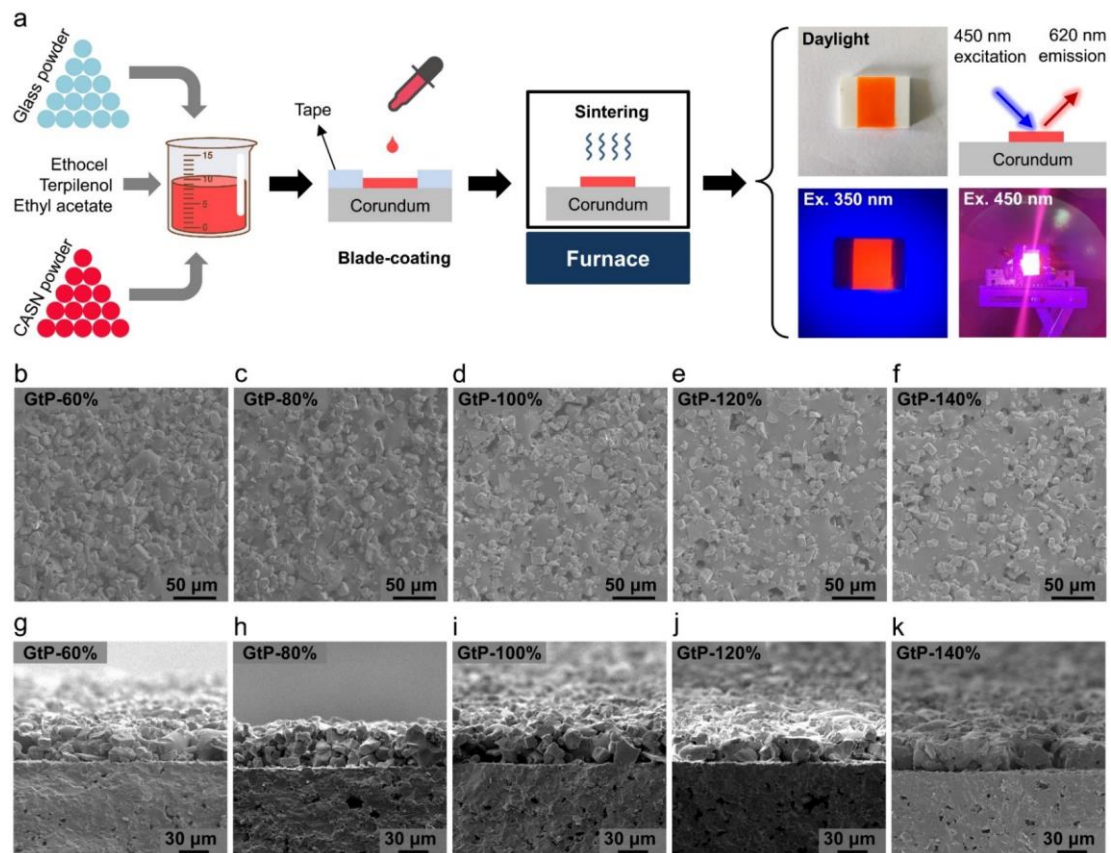
1 ratios were 60%, 80%, 100%, 120%, and 140 %, respectively. The organic vehicle was
2
3 prepared by mixing 0.5 g of ethylcellulose (Aladdin, 98%), 5 mL of ethyl acetate
4
5 (Aladdin, 99.5%) and 2 mL of terpineol (Aladdin, 95%). The viscous ink was printed
6
7 on a corundum (α -Al₂O₃, 99%) substrate ($14 \times 19 \times 2 \text{ mm}^3$) using a blade-coating
8
9 technique. The printed layer was annealed at 120 °C for 3 h to remove all the organics
10
11 and subsequently heated to 470 °C with a heating rate of 5 °C/min (the soaking time is
12
13 zero).
14
15
16
17
18
19
20
21

22 **2.2 Characterization**

23
24
25 The microstructure was observed using a scanning electron microscope (SEM,
26
27 Hitachi, TM-3000 PLUS). The photoluminescence was investigated using a
28
29 spectroradiometer (HORIBA, Fluorolog-3). The luminescence and QE were measured
30
31 using a spectroradiometer (Edinburgh Instruments, FLS-1000) equipped with a 30 cm
32
33 integrating sphere. The QE measurement system has an empirical error of $\pm 3\%$. The
34
35 luminescence saturation behaviors were measured using a home-made sphere-
36
37 spectroradiometer system. The setup for high power mode consists of a 38 W (4.75 W
38
39 $\times 8$, Nichia, NUBM-08) blue LD module, a fiber-coupled integrating sphere with a
40
41 diameter of 15 cm, and an array spectrometer (Instrument Systems, CAS-140-CT-151).
42
43 The spot size of the laser module is $\sim 0.17 \text{ cm}^2$. The setup for high power density mode
44
45 consists of a single 4.5 W blue LD (Nichia, NDB7A75), a fiber-coupled integrating
46
47 sphere (Labsphere, RT-060-SF), and the same array spectrometer (Instrument Systems,
48
49 CAS-140-CT-151). A lens system consisting of a cylindrical lens ($f = 10 \text{ mm}$), a
50
51
52
53
54
55
56
57
58
59
60

1 cylindrical lens ($f = 150$ mm) and an achromatic lens ($f = 200$ mm) was used to shape
 2 and focus the light from the LD. The laser beam profile was captured using a scanning
 3 slit beam profiler (Photon, Beamscan 2180). The output optical power of the blue laser
 4 module was measured using a laser power meter (Ophir, NOVA-II).
 5
 6
 7
 8
 9
 10
 11
 12
 13
 14
 15

16 3. Results



46 **Fig. 1**(a) Fabrication schematic of composite film using the blade-coating method; the digital images
 47 are a typical sample and its lighting effects (when pumped with a UV LED and a blue laser); (b-f) SEM
 48 images of surfaces of composite films with different glass mass ratios; (g-k) SEM images of cross
 49 sections of composite films with different glass mass ratios.
 50
 51
 52
 53
 54
 55
 56

57 **Fig. 1a** shows the fabrication schematic of a composite film (see Section 2.1 for
 58
 59
 60
 61
 62
 63
 64
 65

1 details). The morphologies of composite films were investigated using SEM. The SEM
 2 images of pristine CASN powder and glass powder are shown in Fig. S1. The surface
 3 (top-view) SEM images of composite films in Fig. 1 b-f show that the CASN particles
 4 are well-wetted and embedded in the pore-existing glass matrix. It was found that the
 5 CASN particles are uniformly dispersed in the glass matrix. With increasing GtP ratio,
 6 the porosity gradually decreases. Fig. 1 g-h show the cross-sectional SEM images of
 7 composite films with different glass mass ratios. It was found that the films are tightly
 8 bonded to the corundum substrate, indicating a good adhesion. Notably, the glass mass
 9 ratio can slightly affect the thickness. Fig. S2 shows a clear boundary between the glass
 10 matrix and CASN particle, indicating that no obvious erosion occurs during the heat
 11 treatment. This means the composite films could inherit the high IQE from CASN
 12 powder.

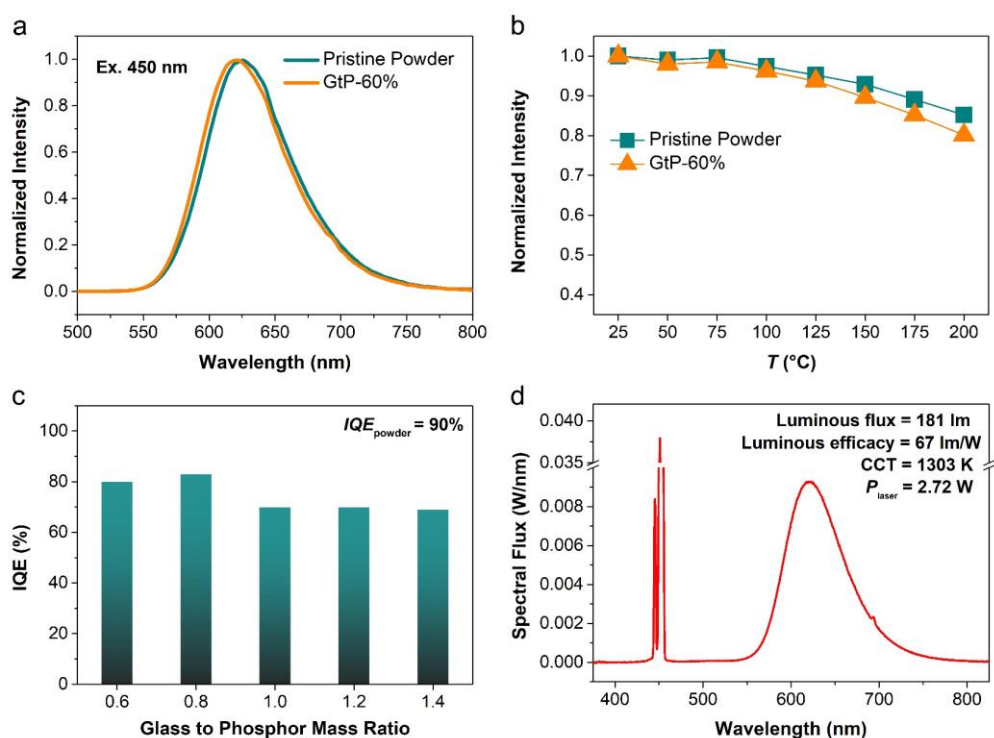
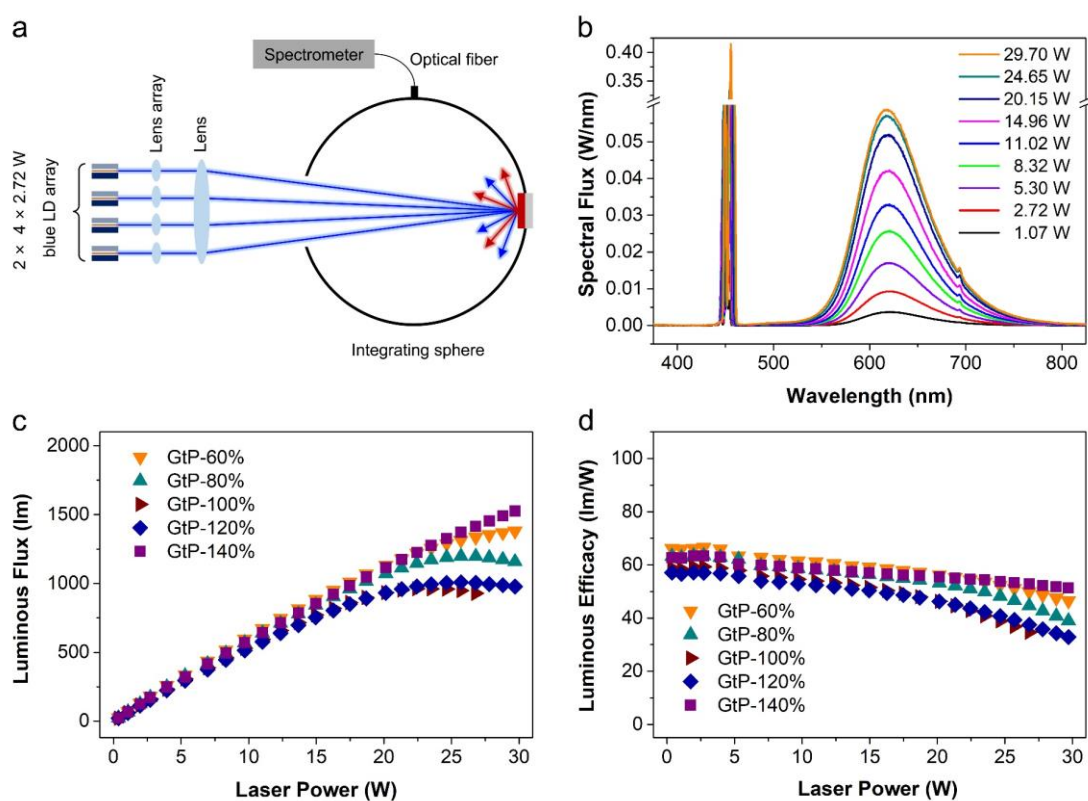


Fig. 2(a) PL mission spectra and (b) thermal quenching behaviors of GtP-60% and pristine powder; (c)

1 IQE of composite films with different GtP; (d) EL spectra of GtP-60% pumped using 2.72 W blue laser
2
3 power.
4
5

6 The optical properties of films are shown in Fig. 2. The excitation spectrum of
7
8 GtP-60% (monitored at 620 nm) is shown in Fig. S3 covering a very broad range of
9
10 250-620 nm, indicating its suitability for combining with blue LDs. The PL emission
11
12 spectra of pristine CASN powder and GtP-60% are shown in Fig. 2a. Under excitation
13
14 of 450 nm, GtP-60% shows a broad and asymmetric emission band with peak at 620
15
16 nm, which can be attributed to the 5d-4f electronic transition of Eu^{2+} . In general, the PL
17
18 profile of GtP-60% is very similar to that of CASN powder. However, a clear blue-shift
19
20 (626 nm \rightarrow 620 nm) is observed, which can be attributed to the mitigated self-
21
22 absorption effect. The luminescence thermal quenching behaviors of pristine powder
23
24 and GtP-60% are shown in Fig. 2b. With the increase of temperature, the lattice
25
26 vibration provides the activation energy for thermally activated cross over (5d to 4f)
27
28 and thermal ionization (5d to conduction band) process. These factors often cause
29
30 decline in IQE and decrease of absorbance [35-37]. Thus, both samples present a
31
32 monotonic decline in PL intensity. GtP-60% inherits the thermal quenching behavior
33
34 from CASN powder; the intensity drop at 200 °C is ~19%. The IQEs of samples (under
35
36 450 nm excitation) with different GtP ratios are shown in Fig. 2c. It was found that the
37
38 GtP ratio significantly affects the IQE. GtP-60% and GtP-80% have a high IQE of 80%
39
40 and 83%, respectively. Subsequently, the IQE continuously decreased with increasing
41
42 GtP ratio. GtP-140% with the highest GtP ratio showed the lowest IQE of ~69%; even
43
44 so it is still an acceptable value. The lower IQE of GtP-140% is probably caused by the
45
46
47
48
49
50
51
52
53
54
55
56
57
58
59
60
61
62
63
64
65

1 elevated corrosion rate resulting from the higher glass ratio. Laser-driven photometric
 2 and colorimetric properties of a typical sample (GtP-60%) were evaluated using a
 3 sphere-spectroradiometer system. Under excitation of 2.72 W (0.13 W/mm^2) blue laser
 4 power (high power mode), GtP-60% provides an intense red emission centered at 622
 5 nm (as shown in Fig. 2d), it yields a high luminous flux of 181 lm (at a CCT of 1303
 6 K); therefore, a high luminous efficacy of 67 lm/W was successfully achieved. These
 7 favorable properties can be attributed to the high IQE ($\sim 80\%$) of the sample.



47 **Fig. 3** (a) Schematic of sphere-spectroradiometer measurement system for high power mode; (b) EL
 48 spectra of GtP-60% pumped with varying laser powers; (c and d) luminous flux and luminous efficacy
 49 of samples with various GtP mass ratio as a function of pumping laser power.

50 Luminescence saturation is a significant obstacle for the development of CASN-
 51 based phosphors for laser lighting. The luminescence saturation behaviors of composite
 52

1 films were systematically evaluated in a very wide laser power range (up to 29.7 W).
2
3 Schematic of sphere-spectroradiometer measurement system for high power mode is
4
5 shown in Fig. 3a. Fig. 3b shows the EL spectra of a typical sample (GtP-60%) pumped
6
7 with an elevated laser power. The EL emission intensity increases monotonously from
8
9 1.07 W to 29.7 W. However, the increase becomes very small from 24.65 W to 29.70
10
11 W, indicating that the saturation threshold is very close. The luminous flux and
12
13 luminous efficacy of different samples as a function of incident laser power are shown
14
15 in Fig. 3c-d. In a low laser power range (<5 W), the GtP ratio slightly affected the
16
17 photometric properties; all the samples exhibited a high luminous efficacy of 57-67
18
19 lm/W. Surprisingly, GtP-140% showed the best robustness; it maintained a high
20
21 luminous efficacy of 51 lm/W even when the incident laser power reached 29.7 W. This
22
23 indicates that it has a remarkably high saturation threshold, and thus an ultrahigh
24
25 luminous flux of 1576 lm could be successfully achieved. Notably, GtP-60% and GtP-
26
27 80% showed a higher IQE ($\geq 80\%$) than GtP-140% ($\sim 69\%$), but their saturation
28
29 thresholds are lower. Theoretically, higher IQE means less conversion loss leading to
30
31 less heat generation. In this case, the heat dissipation capability of sample probably
32
33 plays the major role affecting the saturation threshold. The high porosity of GtP-60%
34
35 and GtP-80% leads to lower thermal dissipation. In contrast, GtP-140% clearly shows
36
37 a lower porosity than the other counterparts. This enables it to effectively remove the
38
39 generated heat and thus achieve the highest saturation threshold. Based on these results,
40
41 GtP-140% is more suitable for laser lighting applications at a high power level (i.e., >20
42
43 W).

1 The luminescence saturation behavior of the GtP-140% was also evaluated in a
2
3 very wide laser power density range (up to 10.2 W/mm^2). Schematic of sphere-
4
5 spectroradiometer measurement system for high power mode is shown in Fig. 4a. The
6
7 variation of the laser power and spot area as a function of driving current were presented
8
9 in Fig. 4b. Notably, the laser spot area increases with the increasing driving current.
10
11 This is attributed to the changing transverse mode at different current, as well as the
12
13 related astigmatism of the blue LD. With the exact spot sizes of the LD at various
14
15 current, the laser power densities on the sample at various laser power were obtained.
16
17 Fig. 4c shows the EL spectra of a typical sample (GtP-140%) pumped with an elevated
18
19 laser power and laser power density. The EL emission intensity increases monotonously
20
21 from 1.87 W/mm^2 to 9.04 W/mm^2 . From 9.04 W/mm^2 to 10.2 W/mm^2 , the intensity
22
23 remained unchanged, indicating the occurrence of luminescence saturation. The
24
25 luminous flux and luminous efficacy of the GtP-140% as a function of incident laser
26
27 power are shown in Fig. 4d. The luminous flux of sample initially increases linearly
28
29 with the increasing incident laser power (laser power density). After 6.56 W/mm^2 (0.58
30
31 W), the increase slows down sharply. The luminous efficacy decreases steadily with the
32
33 increasing incident laser power (laser power density). At 1.87 W/mm^2 (0.04 W), the
34
35 luminous efficacy of the GtP-140% reaches 82 lm/W which is obviously higher than
36
37 the value ($\sim 63 \text{ lm/W}$) measured under high power mode (1.07 W , 0.06 W/mm^2). This
38
39 is probably because of the following two reasons: (1) the single LD (for high power
40
41 density mode) has better monochromaticity and shorter wavelength ($\sim 443 \text{ nm}$, see Fig.
42
43 4c), which is beneficial to improving the absorption of blue light for CASN (see Fig.
44
45
46
47
48
49
50
51
52
53
54
55
56
57
58
59
60
61
62
63
64
65

S3); (2) the lower laser power (0.04 W) for high power density mode leads to less thermal load.

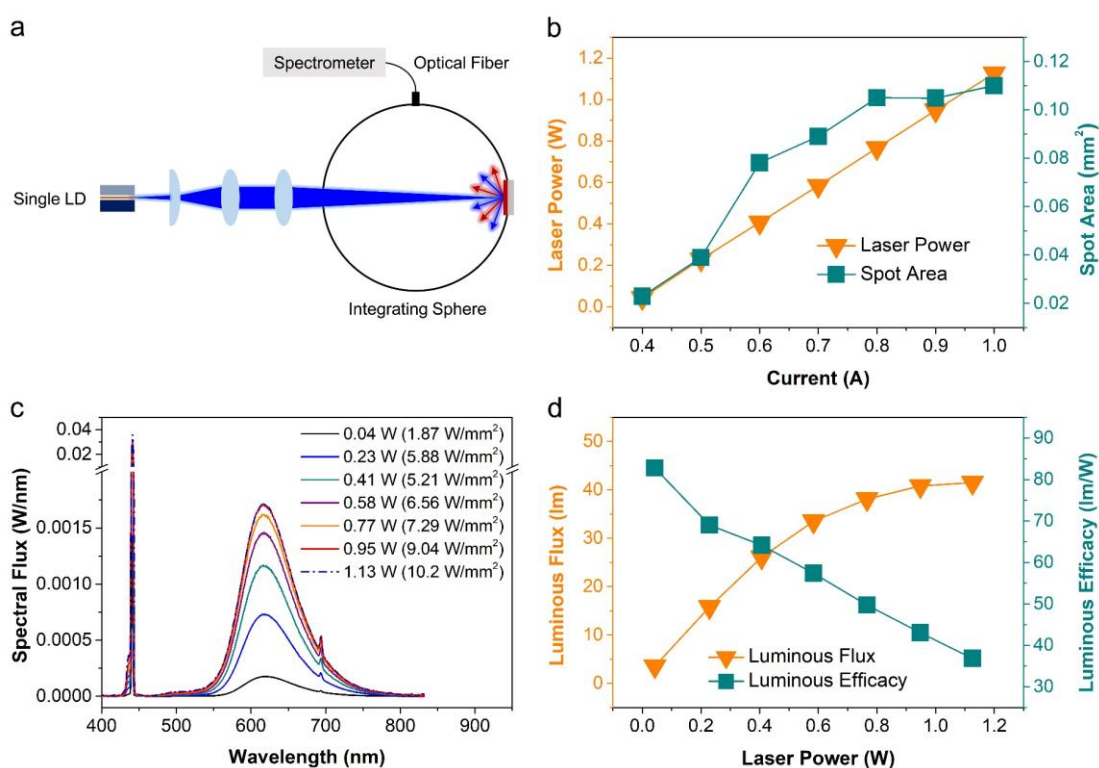


Fig. 4 (a) Schematic of sphere-spectroradiometer measurement system for high power density mode; (b) the variation of the laser power and laser spot area of the single LD as a function of the driving current; (c) EL spectra of GtP-140% pumped with varying laser power; (d) luminous flux and luminous efficacy of GtP-140% as a function of pumping laser power.

Conclusions

A thermally robust and efficient red-emitting composite film was fabricated by cofiring the CASN and glass powders on a corundum substrate. Owing to the low corrosion of SnO-P₂O₅-ZnO glass and the moderate annealing process (470 °C, soaking time is zero), the resulting composite film maintains a high IQE of 83% (92% of that

1 of pristine powder). When pumped with blue laser (1.87 W/mm^2 , 0.04 W), the
2
3 composite film (GtP-140%) attained a record high luminous efficacy of 82 lm/W .
4
5 Furthermore, its saturation threshold was investigated in high power and high power
6
7 density mode, respectively. For high power mode, the GtP-140% shows a saturation
8
9 threshold over 29.7 W (1.75 W/mm^2), thus yielding a high luminous flux of 1576 lm .
10
11 For high power density mode, it shows a saturation threshold of $\sim 10.2 \text{ W/mm}^2$ (1.13
12
13 W). These results suggest that when the laser power reaches to very high level, even
14
15 very low power density can saturate a phosphor. With these favorable properties, we
16
17 believe this study will not only provide a suitable red-emitting phosphor for laser
18
19 lighting, but also provide valuable guidelines for improving the luminous efficacy and
20
21 saturation threshold of other nitride phosphors.
22
23
24
25
26
27
28
29
30
31
32
33

34 **Acknowledgements**

35
36 This work was supported by National Natural Science Foundation of China
37
38 (51802083 and 51772076), Danish Energy Technology Development and
39
40 Demonstration program (EUDP 64017-0588), Natural Science Foundation of
41
42 Fujian/Henan Province ($2019\text{J}05022$, $20\text{A}430018$, 182300410193) and Training plan
43
44 of young backbone teachers in Colleges and Universities of Henan Province
45
46 ($2019\text{GGJS}060$)
47
48
49
50
51
52
53
54
55

56 **References**

57
58 [1] J.J. Wierer, J.Y. Tsao, D.S. Sizov, Comparison between blue lasers and light-
59
60
61
62
63
64
65

- 1 emitting diodes for future solid-state lighting, *Laser & Photonics Reviews* 7 (6)
2
3 (2013) 963-993.
4
5
6 [2] J.J. Wierer Jr, J.Y. Tsao, D.S. Sizov, The potential of III-nitride laser diodes for
7
8 solid-state lighting, *Physica Status Solidi C* 11 (3- 4) (2014) 674-677.
9
10
11 [3] N. Trivellin, M. Yushchenko, M. Buffolo, C. De Santi, M. Meneghini, G.
12
13 Meneghesso, E. Zanoni, *Laser-Based Lighting: Experimental Analysis and*
14
15 *Perspectives*, *Materials* 10 (10) (2017) 1166.
16
17
18 [4] S. Li, L. Wang, N. Hirosaki, R.J. Xie, Color Conversion Materials for High-
19
20 Brightness Laser- Driven Solid- State Lighting, *Laser & Photonics Reviews* 12 (12)
21
22 (2018) 1800173.
23
24
25 [5] A. Pourhashemi, R. Farrell, M. Hardy, P.S. Hsu, K. Kelchner, J. Speck, S.
26
27 Denbaars, S. Nakamura, Pulsed high-power AlGaN-cladding-free blue laser diodes on
28
29 semipolar (2021) GaN substrates, *Applied Physics Letters* 103 (2013) 1112.
30
31
32 [6] L. Wang, R.-J. Xie, T. Suehiro, T. Takeda, N. Hirosaki, *Down-Conversion Nitride*
33
34 *Materials for Solid State Lighting: Recent Advances and Perspectives*, *Chemical*
35
36 *Reviews* 118 (4) (2018) 1951-2009.
37
38
39 [7] H. Lin, T. Hu, Y. Cheng, M. Chen, Y. Wang, *Glass Ceramic Phosphors: Towards*
40
41 *Long-Lifetime High-Power White Light-Emitting-Diode Applications—A Review*,
42
43 *Laser & Photonics Reviews* 12 (6) (2018) 1700344.
44
45
46 [8] J. Xu, Y. Yang, Z. Guo, D.D. Corell, B. Du, B. Liu, H. Ji, C. Dam-Hansen, O.B.
47
48 Jensen, Comparative study of Al₂O₃-YAG:Ce composite ceramic and single crystal
49
50 YAG:Ce phosphors for high-power laser lighting, *Ceramics International* 46 (11)
51
52
53
54
55
56
57
58
59
60
61
62
63
64
65

1 (2020) 17923-17928.

2
3 [9] J. Xu, J. Wang, Y. Gong, X. Ruan, Z. Liu, B. Hu, B. Liu, H. Li, X. Wang, B. Du,
4
5
6 Investigation of an LuAG:Ce translucent ceramic synthesized via spark plasma
7
8
9 sintering: Towards a facile synthetic route, robust thermal performance, and high-
10
11 power solid state laser lighting, *Journal of the European Ceramic Society* 38 (1)
12
13 (2018) 343-347.

14
15
16 [10] Q.-Q. Zhu, X.-J. Wang, L. Wang, N. Hirosaki, T. Nishimura, Z.-F. Tian, Q. Li, Y.-
17
18
19 Z. Xu, X. Xu, R.-J. Xie, β -Sialon:Eu phosphor-in-glass: a robust green color converter
20
21
22 for high power blue laser lighting, *Journal of Materials Chemistry C* 3 (41) (2015)
23
24
25 10761-10766.

26
27
28 [11] H. Wu, Z. Hao, G.-H. Pan, L. Zhang, H. Wu, X. Zhang, L. Zhang, J. Zhang,
29
30
31 Phosphor-SiO₂ composite films suitable for white laser lighting with excellent color
32
33
34 rendering, *Journal of the European Ceramic Society* 40 (6) (2020) 2439-2444.

35
36 [12] Y. Zhang, Z. Zhang, X. Liu, G. Shao, L. Shen, J. Liu, W. Xiang, X. Liang, A high
37
38
39 quantum efficiency CaAlSiN₃:Eu²⁺ phosphor-in-glass with excellent optical
40
41
42 performance for white light-emitting diodes and blue laser diodes, *Chemical*
43
44
45 *Engineering Journal* 401 (2020) 125983.

46
47 [13] J. Xu, A. Thorseth, C. Xu, A. Krasnoshchoka, M. Rosendal, C. Dam-Hansen, B.
48
49
50 Du, Y. Gong, O.B. Jensen, Investigation of laser-induced luminescence saturation in a
51
52
53 single-crystal YAG:Ce phosphor: Towards unique architecture, high saturation
54
55
56 threshold, and high-brightness laser-driven white lighting, *Journal of Luminescence*
57
58
59 212 (2019) 279-285.

- 1 [14] R. Wei, L. Wang, P. Zheng, H. Zeng, G. Pan, H. Zhang, P. Liang, T. Zhou, R. Xie,
2
3 On the luminance saturation of phosphor-in-glass (PiG) films for blue-laser-driven
4
5 white lighting: Effects of the phosphor content and the film thickness, Journal of the
6
7 European Ceramic Society 39 (5) (2019) 1909-1917.
8
9
10
11 [15] P. Zheng, S. Li, L. Wang, T.L. Zhou, S. You, T. Takeda, N. Hirosaki, R.J. Xie,
12
13 Unique Color Converter Architecture Enabling Phosphor-in-Glass (PiG) Films
14
15 Suitable for High-Power and High-Luminance Laser-Driven White Lighting, ACS
16
17 applied materials & interfaces 10 (17) (2018) 14930-14940.
18
19
20
21 [16] P. Zheng, S. Li, R. Wei, L. Wang, T.L. Zhou, Y.R. Xu, T. Takeda, N. Hirosaki,
22
23 R.J. Xie, Unique Design Strategy for Laser- Driven Color Converters Enabling
24
25 Superhigh- Luminance and High- Directionality White Light, Laser & Photonics
26
27 Reviews 13 (10) (2019) 1900147.
28
29
30
31 [17] Y. Yuan, D. Wang, B. Zhou, S. Feng, M. Sun, S. Zhang, W. Gao, Y. Bi, H. Qin,
32
33 High luminous fluorescence generation using Ce:YAG transparent ceramic excited by
34
35 blue laser diode, Optical Materials Express 8 (9) (2018) 2760.
36
37
38
39 [18] A. Krasnoshchoka, A. Thorseth, C. Dam-Hansen, D.D. Corell, P.M. Petersen,
40
41 O.B. Jensen, Investigation of Saturation Effects in Ceramic Phosphors for Laser
42
43 Lighting, Materials (Basel) 10 (12) (2017).
44
45
46
47 [19] Q. Yao, P. Hu, P. Sun, M. Liu, R. Dong, K. Chao, Y. Liu, J. Jiang, H. Jiang,
48
49 YAG:Ce³⁺ Transparent Ceramic Phosphors Brighten the Next-Generation Laser-
50
51 Driven Lighting, Advanced materials 32 (19) (2020) e1907888.
52
53
54
55 [20] Q.-Q. Zhu, Y. Meng, H. Zhang, S. Li, L. Wang, R.-J. Xie, YAGG:Ce Phosphor-
56
57
58
59
60
61
62
63
64
65

1 in-YAG Ceramic: An Efficient Green Color Converter Suitable for High-Power Blue
2
3 Laser Lighting, ACS Applied Electronic Materials 2 (8) (2020) 2644-2650.
4

5
6 [21] K. Li, Y. Shi, F. Jia, C. Price, Y. Gong, J. Huang, N. Copner, H. Cao, L. Yang, S.
7
8 Chen, Low Etendue Yellow-Green Solid-State Light Generation by Laser-pumped
9
10 LuAG:Ce Ceramic, IEEE Photonics Technology Letters 30 (10) (2018) 1-1.
11

12
13 [22] P. Sun, P. Hu, Y. Liu, S. Liu, R. Dong, J. Jiang, H. Jiang, Broadband emissions
14
15 from $\text{Lu}_2\text{Mg}_2\text{Al}_2\text{Si}_2\text{O}_{12}:\text{Ce}^{3+}$ plate ceramic phosphors enable a high color-rendering
16
17 index for laser-driven lighting, Journal of Materials Chemistry C 8 (4) (2020) 1405-
18
19
20
21
22 1412.
23

24
25 [23] X. Liu, X. Qian, Z. Hu, X. Chen, Y. Shi, J. Zou, J. Li, $\text{Al}_2\text{O}_3\text{-Ce:GdYAG}$
26
27 composite ceramic phosphors for high-power white light-emitting-diode applications,
28
29
30
31 Journal of the European Ceramic Society 39 (6) (2019) 2149-2154.
32

33
34 [24] S. Li, Q. Zhu, D. Tang, X. Liu, G. Ouyang, L. Cao, N. Hirosaki, T. Nishimura, Z.
35
36 Huang, R.-J. Xie, $\text{Al}_2\text{O}_3\text{-YAG:Ce}$ composite phosphor ceramic: a thermally robust
37
38 and efficient color converter for solid state laser lighting, Journal of Materials
39
40
41
42
43
44
45
46
47
48
49
50
51
52
53
54
55
56
57
58
59
60
61
62
63
64
65

66
67 [25] C. Cozzan, G. Lheureux, N. O'Dea, E.E. Levin, J. Graser, T.D. Sparks, S.
68
69 Nakamura, S.P. DenBaars, C. Weisbuch, R. Seshadri, Stable, Heat-Conducting
70
71
72
73
74
75
76
77
78
79
80
81
82
83
84
85
86
87
88
89
90
91
92
93
94
95
96
97
98
99
100
101
102
103
104
105
106
107
108
109
110
111
112
113
114
115
116
117
118
119
120
121
122
123
124
125
126
127
128
129
130
131
132
133
134
135
136
137
138
139
140
141
142
143
144
145
146
147
148
149
150
151
152
153
154
155
156
157
158
159
160
161
162
163
164
165
166
167
168
169
170
171
172
173
174
175
176
177
178
179
180
181
182
183
184
185
186
187
188
189
190
191
192
193
194
195
196
197
198
199
200
201
202
203
204
205
206
207
208
209
210
211
212
213
214
215
216
217
218
219
220
221
222
223
224
225
226
227
228
229
230
231
232
233
234
235
236
237
238
239
240
241
242
243
244
245
246
247
248
249
250
251
252
253
254
255
256
257
258
259
260
261
262
263
264
265
266
267
268
269
270
271
272
273
274
275
276
277
278
279
280
281
282
283
284
285
286
287
288
289
290
291
292
293
294
295
296
297
298
299
300
301
302
303
304
305
306
307
308
309
310
311
312
313
314
315
316
317
318
319
320
321
322
323
324
325
326
327
328
329
330
331
332
333
334
335
336
337
338
339
340
341
342
343
344
345
346
347
348
349
350
351
352
353
354
355
356
357
358
359
360
361
362
363
364
365
366
367
368
369
370
371
372
373
374
375
376
377
378
379
380
381
382
383
384
385
386
387
388
389
390
391
392
393
394
395
396
397
398
399
400
401
402
403
404
405
406
407
408
409
410
411
412
413
414
415
416
417
418
419
420
421
422
423
424
425
426
427
428
429
430
431
432
433
434
435
436
437
438
439
440
441
442
443
444
445
446
447
448
449
450
451
452
453
454
455
456
457
458
459
460
461
462
463
464
465
466
467
468
469
470
471
472
473
474
475
476
477
478
479
480
481
482
483
484
485
486
487
488
489
490
491
492
493
494
495
496
497
498
499
500
501
502
503
504
505
506
507
508
509
510
511
512
513
514
515
516
517
518
519
520
521
522
523
524
525
526
527
528
529
530
531
532
533
534
535
536
537
538
539
540
541
542
543
544
545
546
547
548
549
550
551
552
553
554
555
556
557
558
559
560
561
562
563
564
565
566
567
568
569
570
571
572
573
574
575
576
577
578
579
580
581
582
583
584
585
586
587
588
589
590
591
592
593
594
595
596
597
598
599
600
601
602
603
604
605
606
607
608
609
610
611
612
613
614
615
616
617
618
619
620
621
622
623
624
625
626
627
628
629
630
631
632
633
634
635
636
637
638
639
640
641
642
643
644
645
646
647
648
649
650
651
652
653
654
655
656
657
658
659
660
661
662
663
664
665
666
667
668
669
670
671
672
673
674
675
676
677
678
679
680
681
682
683
684
685
686
687
688
689
690
691
692
693
694
695
696
697
698
699
700
701
702
703
704
705
706
707
708
709
710
711
712
713
714
715
716
717
718
719
720
721
722
723
724
725
726
727
728
729
730
731
732
733
734
735
736
737
738
739
740
741
742
743
744
745
746
747
748
749
750
751
752
753
754
755
756
757
758
759
760
761
762
763
764
765
766
767
768
769
770
771
772
773
774
775
776
777
778
779
780
781
782
783
784
785
786
787
788
789
790
791
792
793
794
795
796
797
798
799
800
801
802
803
804
805
806
807
808
809
810
811
812
813
814
815
816
817
818
819
820
821
822
823
824
825
826
827
828
829
830
831
832
833
834
835
836
837
838
839
840
841
842
843
844
845
846
847
848
849
850
851
852
853
854
855
856
857
858
859
860
861
862
863
864
865
866
867
868
869
870
871
872
873
874
875
876
877
878
879
880
881
882
883
884
885
886
887
888
889
890
891
892
893
894
895
896
897
898
899
900
901
902
903
904
905
906
907
908
909
910
911
912
913
914
915
916
917
918
919
920
921
922
923
924
925
926
927
928
929
930
931
932
933
934
935
936
937
938
939
940
941
942
943
944
945
946
947
948
949
950
951
952
953
954
955
956
957
958
959
960
961
962
963
964
965
966
967
968
969
970
971
972
973
974
975
976
977
978
979
980
981
982
983
984
985
986
987
988
989
990
991
992
993
994
995
996
997
998
999
1000

1 performance, and application in solid-state laser lighting, *Optical Materials* 75 (2018)
2
3 508-512.

4
5
6 [27] V. Bachmann, C. Ronda, A. Meijerink, Temperature Quenching of Yellow Ce^{3+}
7
8 Luminescence in YAG:Ce, *Chemistry of Materials* 21 (10) (2009) 2077-2084.

9
10
11 [28] J. Xu, Y. Yang, Z. Guo, B. Hu, J. Wang, B. Du, B. Liu, H. Ji, C. Dam-Hansen,
12
13 O.B. Jensen, Design of a $\text{CaAlSiN}_3\text{:Eu}$ /glass composite film: Facile synthesis, high
14
15 saturation-threshold and application in high-power laser lighting, *Journal of the*
16
17
18
19
20
21
22
23
24
25
26
27
28
29
30
31
32
33
34
35
36
37
38
39
40
41
42
43
44
45
46
47
48
49
50
51
52
53
54
55
56
57
58
59
60
61
62
63
64
65

European Ceramic Society 40 (13) (2020) 4704-4708.

[29] Q.-Q. Zhu, X. Xu, L. Wang, Z.-F. Tian, Y.-Z. Xu, N. Hirosaki, R.-J. Xie, A robust
red-emitting phosphor-in-glass (PiG) for use in white lighting sources pumped by
blue laser diodes, *Journal of Alloys and Compounds* 702 (2017) 193-198.

[30] S. Li, Q. Zhu, L. Wang, D. Tang, Y. Cho, X. Liu, N. Hirosaki, T. Nishimura, T.
Sekiguchi, Z. Huang, R.-J. Xie, $\text{CaAlSiN}_3\text{:Eu}^{2+}$ translucent ceramic: a promising
robust and efficient red color converter for solid state laser displays and lighting,
Journal of Materials Chemistry C 4 (35) (2016) 8197-8205.

[31] Z. Lin, H. Lin, J. Xu, F. Huang, H. Chen, B. Wang, Y. Wang, Highly thermal-
stable warm w-LED based on Ce:YAG PiG stacked with a red phosphor layer, *Journal*
of Alloys and Compounds 649 (2015) 661-665.

[32] T. Jansen, D. Böhnisch, T. Jüstel, On the Photoluminescence Linearity of Eu^{2+}
Based LED Phosphors upon High Excitation Density, *ECS Journal of Solid State*
Science and Technology 5 (6) (2016) R91-R97.

[33] S. Li, D. Tang, Z. Tian, X. Liu, T. Takeda, N. Hirosaki, F. Xu, Z. Huang, R.J.

1 Xie,, New insights into the microstructure of translucent CaAlSiN₃:Eu²⁺ phosphor
2
3 ceramics for solid-state laser lighting, Journal of Materials Chemistry C Materials for
4
5 Optical & Electronic Devices 5 (2017) 1042-1051
6
7
8
9 [34] S. Li, L. Wang, D. Tang, Y. Cho, X. Liu, X. Zhou, L. Lu, L. Zhang, T. Takeda, N.
10
11 Hirosaki, R.-J. Xie, Achieving High Quantum Efficiency Narrow-Band β-Sialon:Eu²⁺
12
13 Phosphors for High-Brightness LCD Backlights by Reducing the Eu³⁺ Luminescence
14
15 Killer, Chemistry of Materials 30 (2) (2017) 494-505.
16
17
18
19 [35] J. Ueda, P. Dorenbos, A.J.J. Bos, A. Meijerink, S. Tanabe, Insight into the
20
21 Thermal Quenching Mechanism for Y₃Al₅O₁₂:Ce³⁺ through Thermoluminescence
22
23 Excitation Spectroscopy, The Journal of Physical Chemistry C 119 (44) (2015) 25003-
24
25 25008.
26
27
28
29 [36] J. Ueda, S. Tanabe, K. Takahashi, T. Takeda, N. Hirosaki, Thermal Quenching
30
31 Mechanism of CaAlSiN₃:Eu²⁺ Red Phosphor, Bulletin of the Chemical Society of Japan
32
33
34 91 (2) (2018) 173-177.
35
36
37
38
39 [37] Y. Liu, J. Silver, R.-J. Xie, J. Zhang, H. Xu, H. Shao, J. Jiang, H. Jiang, An
40
41 excellent cyan-emitting orthosilicate phosphor for NUV-pumped white LED
42
43 application, Journal of Materials Chemistry C 5 (47) (2017) 12365-12377.
44
45
46
47
48
49
50
51
52
53
54
55
56
57
58
59
60
61
62
63
64
65